

PAPER • OPEN ACCESS

Photoproduction of J/ψ in non-single-diffractive $p+p$ collisions

To cite this article: Ze-Hua Cao *et al* 2019 *Chinese Phys. C* **43** 064103

View the [article online](#) for updates and enhancements.

You may also like

- [Charmonia and bottomonia in asymmetric magnetized hot nuclear matter](#)
Rajesh Kumar and Arvind Kumar
- [Study of the \$a_1\(1260\)\$ resonance in the \$p^{++}\$ reaction](#)
Xu Zhang, , Ju-Jun Xie et al.
- [Response functions of hot and dense matter in the Nambu-Jona-Lasinio model](#)
Chengfu Mu, , Ziyue Wang et al.

Photoproduction of J/ψ in non-single-diffractive p+p collisions*

Ze-Hua Cao(曹泽华)^{1,2} Li-Juan Ruan(阮丽娟)³ Ze-Bo Tang(唐泽波)^{1,2} Zhang-Bu Xu(许长补)^{3,4}

Chi Yang(杨驰)⁴ Shuai Yang(杨帅)³ Wang-Mei Zha(查王妹)^{1,2,1)}

¹State Key Laboratory of Particle Detection and Electronics, University of Science and Technology of China, Hefei 230026, China

²Department of Modern Physics, University of Science and Technology of China, Hefei 230026, China

³Brookhaven National Laboratory, New York, USA

⁴Shandong University, Jinan 250100, China

Abstract: Significant enhancements of J/ψ production at very low transverse momenta were recently observed by the ALICE and STAR collaborations in peripheral hadronic A+A collisions. The anomalous excess points to coherent photon-nucleus interactions in violent hadronic heavy-ion collisions, which were conventionally studied only in ultra-peripheral collisions. Assuming that the coherent photoproduction is the underlying mechanism responsible for the excess observed in peripheral A+A collisions, its contribution in p+p collisions with nuclear overlap, i.e. non-single-diffractive collisions, is of particular interest. In this paper, we perform a calculation of exclusive J/ψ photoproduction in non-single-diffractive p+p collisions at the RHIC and LHC energies based on the pQCD motivated parametrization using the world-wide experimental data, which could be further employed to improve the precision of the phenomenological calculations for photoproduction in A+A collisions. The differential rapidity and transverse momentum distributions of J/ψ from photoproduction are presented. In comparison with the J/ψ production from hadronic interactions, we find that the contribution of photoproduction is negligible.

Keywords: photoproduction, jpsi, RHIC, LHC

PACS: 25.20.Lj, 25.75.Dw **DOI:** 10.1088/1674-1137/43/6/064103

1 Introduction

In ultra-relativistic heavy-ion collisions, the aim is the search for a new form of matter - the Quark-Gluon Plasma (QGP), which was predicted by the lattice Quantum Chromodynamics (QCD) calculation [1], and the study of its properties in laboratory [2-4]. Among the probes of QGP, J/ψ suppression in hadronic heavy-ion collisions with respect to elementary p+p collisions has been suggested as a “smoking gun” signature of QGP formation [5] due to the color screening effect in the deconfined medium. J/ψ can also be generated by the intense electromagnetic fields that accompany the relativistic heavy ions via coherent photoproduction [6]. The coherently produced J/ψ are expected to probe the nuclear gluon distribution at low Bjorken- x [7], for which there is still a considerable uncertainty [8]. Conventionally, the associated

physics of the J/ψ photoproduction and hadronic production belong to different subject fields, and they are studied in ultra-peripheral collisions (UPC) and hadronic collisions independently. In UPC, only photoproduction and related physics is studied, since there is no hadronic interaction; analogously, in hadronic collisions, only hadronic production is expected.

Is coherent photoproduction really prohibited in hadronic collisions, where violent strong interactions occur? Recently, a significant excess of J/ψ production at very low transverse momentum ($p_T < 0.3$ GeV/c) was observed by the ALICE collaboration in peripheral hadronic Pb+Pb collisions at forward-rapidity [9], which can not be described by the hadronic production that is modified by the hot and cold medium effects. STAR made the same measurements in Au+Au collisions at $\sqrt{s_{NN}} = 200$ GeV and U+U collisions at $\sqrt{s_{NN}} = 193$ GeV [10], and

Received 26 October 2018, Revised 20 January 2019, Published online 23 April 2019

* Supported by the National Natural Science Foundation of China (11775213, 11505180, 11675168), the U.S. DOE Office of Science (DE-SC0012704) and MOST (2016YFE0104800)

1) E-mail: first@ustc.edu.cn



Content from this work may be used under the terms of the Creative Commons Attribution 3.0 licence. Any further distribution of this work must maintain attribution to the author(s) and the title of the work, journal citation and DOI. Article funded by SCOAP3 and published under licence by Chinese Physical Society and the Institute of High Energy Physics of the Chinese Academy of Sciences and the Institute of Modern Physics of the Chinese Academy of Sciences and IOP Publishing Ltd

also observed significant enhancements at very low p_T in peripheral collision. The observed excesses exhibit the characteristics of coherent photoproduction and can be quantitatively explained by the theoretical calculations with coherent photon-nucleus production mechanism [11–13], which strongly suggests the existence of coherent photoproduction in hadronic collisions. If coherent photoproduction is the underlying mechanism responsible for the observed excesses in the hadronic A+A collisions, what is its contribution in hadronic p+p collisions? Can we observe the excess that originates from the same production mechanism in hadronic p+p collisions? If the contribution is significant, it would affect the pp baseline used for nuclear modification factor (R_{AA}) of J/ψ , which would further bias our understanding of QGP extracted from J/ψ suppression measurements. In this paper, we perform a calculation of exclusive J/ψ photoproduction in non-single-diffractive (NSD) p+p collisions at the RHIC and LHC energies. The differential rapidity and transverse momentum distributions of J/ψ from photoproduction are presented, and are compared to those from hadronic production.

2 Methodology

According to the equivalent photon approximation, the photoproduction rate in p+p collisions can be factorized into two parts: the photon flux, and the photon-proton cross-section. The cross-section can be written as:

$$\sigma(p+p \rightarrow p+p+J/\psi) = \int d\omega n(\omega) \sigma(\gamma p \rightarrow J/\psi p), \quad (1)$$

where ω is the photon energy, $n(\omega)$ is the photon flux at energy ω , and $\sigma(\gamma p \rightarrow J/\psi p)$ is the photonuclear interaction cross-section for J/ψ . For simplicity, to make an estimate of its contribution, we assume that the photoproduction process in non-single-diffractive p+p collisions is exactly the same as in UPC.

The photon flux induced by a proton can be modeled using the Weizsäcker-Williams method [14]. For the point-like charge distribution, the photon flux is given by the simple formula

$$n(\omega, r) = \frac{d^3N}{d\omega d^2r} = \frac{Z^2 \alpha}{\pi^2 \omega r^2} x^2 K_1^2(x), \quad (2)$$

where $n(\omega, r)$ is the flux of photons with energy ω at distance r from the center of a proton, α is the electromagnetic coupling constant, $x = \omega r / \gamma$, and γ is the Lorentz factor. Here, K_1 is a modified Bessel function. The point-like assumption is appropriate in UPC. However, in NSD collisions, the two colliding protons come very close to each other and the proton internal structure should be taken into account. A generic formula for any charge distribution can be written as [14]:

$$n(\omega, r) = \frac{4Z^2 \alpha}{\omega} \left| \int \frac{d^2q_\perp}{(2\pi)^2} q_\perp \frac{F(q)}{q^2} e^{iq_\perp r} \right|^2, \quad (3)$$

$$q = \left(q_\perp, \frac{\omega}{\gamma} \right),$$

where the form-factor $F(q)$ is the Fourier transform of the internal charge distribution in a proton. A dipole form is employed to describe the form-factor of a proton, defined as:

$$F(q) = \left(1 + \frac{q^2}{a^2} \right)^{-2}, \quad (4)$$

where the parameter a is related to the root mean square charge radius of the proton ($r_p: 0.8768 \pm 0.0069$ fm [15])

by the equation $a = \frac{\sqrt{12} \hbar c}{r_p}$. Figure 1 shows the two-dimensional distribution of the photon flux induced in p+p collisions at $\sqrt{s} = 200$ GeV as a function of distance r and energy ω with the dipole form-factor for the proton. One can observe that the photon flux drops rapidly as $r \rightarrow 0$ inside the proton.

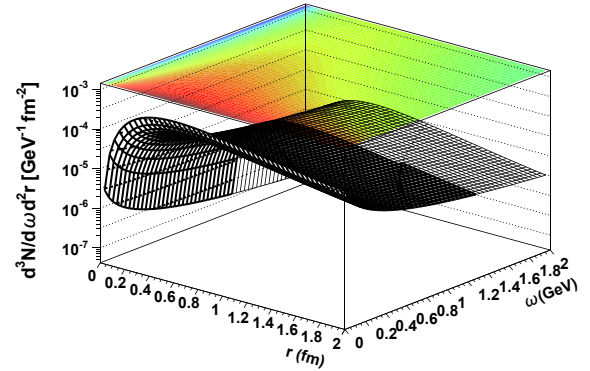


Fig. 1. (color online) Two-dimensional distribution of the photon flux as function of the distance r and the energy of the photon ω for p+p collisions at $\sqrt{s} = 200$ GeV

The photoproduction cross-section $\sigma(\gamma p \rightarrow J/\psi p)$ depends on the gluon density in the proton [16]. At mid-rapidity, J/ψ production is sensitive to gluons with x down to 1.5×10^{-2} at RHIC and 6×10^{-4} at the LHC. However, there is still a large uncertainty in such a region of x for different PDF sets. In this calculation, we use the world-wide experimental data [17–34] for the exclusive J/ψ photoproduction to perform a parametrization of the cross-section estimates. The measurements of J/ψ photoproduction have been performed for more than forty years. In such a long period, different experimental techniques have been utilized and different input information was available at the time of measurements. For example, the branching ratios of $J/\psi \rightarrow e^+e^-$ or $(\mu^+\mu^-)$ have changed with time. To compare different experimental results on equal footing, all measurements are updated with the latest branching fractions ($5.961 \pm 0.032\%$ for

$J/\psi \rightarrow e^+ + e^-$, $5.971 \pm 0.032\%$ for $J/\psi \rightarrow \mu^+ + \mu^-$ [35]. In Ref. [25-27,29-34], the cross-section $\sigma(\gamma p \rightarrow J/\psi p)$ is derived from the measurements of γA using the relation $\frac{d\sigma}{dt}(\gamma + p)|_{t=0} = \frac{1}{A^2} \frac{d\sigma}{dt}(\gamma + A)|_{t=0}$ with the information for $\frac{d\sigma}{dt}(\gamma + p)$ distribution from the world-wide measurements, where t is the four-momentum transfer in the process. One should be aware that the effects of nuclear breakup, proton excitation and the potential phase factor are neglected in the extrapolation process, which needs to be further investigated in a future effort. The cross-section so obtained as a function of γp center-of-mass energy ($E_{\gamma p}$) is shown in Fig. 2. The data are fitted using the following pQCD motivated expression [36]:

$$\sigma(E_{\gamma p}) = C_0 \left(1 - \frac{(m_p + M_{J/\psi})^2}{E_{\gamma p}^2} \right)^{1.5} \left(\frac{E_{\gamma p}^2}{100^2 \text{GeV}^2} \right)^\delta, \quad (5)$$

where the second term on the right-hand side of the equation represents the turning on action near the production threshold, and the last term contains the evolution of gluon distribution on the Bjorken- x . The values of the free parameters C_0 and δ are determined from the fit, resulting in $C_0 = 80.2 \pm 0.9$ nb and $\delta = 0.321 \pm 0.005$. The systematic uncertainties of the measurements from the same experiment must be highly correlated, however the correlation matrix could not be obtained from the corresponding references. Therefore the correlations are not included in the fit, which would underestimate the error bars of C_0 and δ . The parametrization with the most complete experimental data could also be employed to improve the precision of phenomenological calculations for photoproduction in A+A collisions such as in [11-13,37,38]. As shown in the figure, the parametrization describes the experimental measurements very well with $\chi^2/NDF = 113.6/116$. The references of the data are summarized in Table 1.

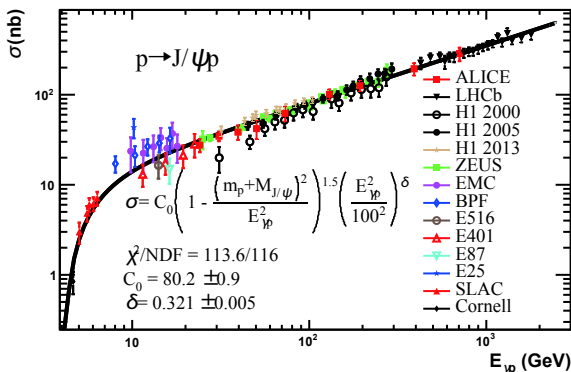


Fig. 2. (color online) Exclusive J/ψ photoproduction cross-section as a function of $E_{\gamma p}$ from the world-wide experimental measurements. The black solid line with the gray band on top of it represents the parametrization discussed in the text.

Table 1. Summary of references for the world-wide data.

experiment	σ	b	collision system
ALICE	[17,18]		p-Pb/pp
LHCb	[19,20]	[20]	PP
H1(2013)	[21]	[21]	ep
H1(2005)	[22]	[22]	ep
H1(2000)	[23]	[23]	ep
ZEUS	[24]	[24]	ep
EMC	[25]	[25]	μ Fe
BPF	[26,27]		μ Fe
E516	[28]	[28]	γ p
E401	[29]	[29]	γ p/d
E87	[30,31]		γ Be
E25	[32]	[32]	γ d
SLAC	[33]		γ d
cornell	[34]		γ Be

To effectively relate the NSD cross-section to its corresponding region in the impact parameter space, a Glauber like geometrical picture is employed in the calculations:

$$\sigma_{\text{NSD}} = \int_0^\infty 2\pi b P_{\text{NSD}}(b) db, \quad (6)$$

$$P_{\text{NSD}}(b) = \int d^2 s T(\vec{s}) (1 - e^{-\sigma_0 T(\vec{s}-\vec{b})}),$$

where $P_{\text{NSD}}(b)$ is the NSD probability as a function of the impact parameter b , $T(\vec{s}) = \int_{-\infty}^{+\infty} dz \rho(r = \sqrt{s^2 + z^2})$ is the density distribution for a proton in the transverse plane, and σ_0 is the cross-section like parameter determined by the NSD cross-section. The density distribution for a proton is given by:

$$\rho(r) = \rho^0 e^{-ar}, \quad (7)$$

where ρ^0 is the normalization factor. The parametrization formula for the density distribution is consistent with the dipole form-factor given in Eq. (4). There are two components in NSD interactions: colored hadronic interactions, and double-diffractive (DD) interactions. The two classes of interactions have different impact parameters. However, for simplicity, we do not make a distinction between these two types of interactions here, which needs to be further investigated in a future work. In this paper, we perform calculations for NSD p+p collisions at $\sqrt{s} = 0.2, 2.76, 5.02$ TeV, and 14 TeV. The corresponding NSD cross-sections are 30, 50, 56, and 64 mb [39], respectively.

3 Results

With the convolution of equivalent photon spectra and elementary $\gamma p \rightarrow J/\psi p$ cross-section, the probability to produce a J/ψ with rapidity y in a collision with an impact parameter b can be given by:

$$\frac{dP(y,b)}{dy} = \omega N(\omega,b) \sigma_{\gamma p \rightarrow J/\psi p}(E_{\gamma p}), \quad (8)$$

where $N(\omega,b)$ is the effective photon flux with an impact parameter b at photon energy ω . The effective photon flux, $N(\omega,b)$, can be expressed by the photon flux induced by one proton and the effective strength for a photon with a second proton:

$$N(\omega,b) = \int n(\omega,r) \frac{\theta(r_p - (|\vec{r} - \vec{b}|))}{\pi r_p^2} d^2r, \quad (9)$$

where b is the impact parameter between the two colliding protons, r is the distance from the proton which emits the photon, and the extra $\theta(r_p - (|\vec{r} - \vec{b}|))$ ensures a collision between the photon and the proton. The photon energy, ω , can be determined from the rapidity of J/ψ , y :

$$\omega = \frac{1}{2} M_{J/\psi} e^y. \quad (10)$$

A complication is that either beam particle is equally likely to produce the photon; the cross-sections for these two possibilities from two beam directions are added:

$$\frac{d\sigma}{dy} = \int_0^\infty \left(\frac{dP(y,b)}{dy} + \frac{dP(-y,b)}{dy} \right) P_{\text{NSD}}(b) 2\pi b db, \quad (11)$$

where $P_{\text{NSD}}(b)$ can be obtained from Eq. (6). Figure 3 shows the calculated rapidity distribution $d\sigma/dy$ of produced J/ψ from photoproduction in NSD p+p collisions at $\sqrt{s} = 200$ GeV. The solid line is the total production cross-section, while the dashed/dotted lines represent individual contributions from the two beam protons. The

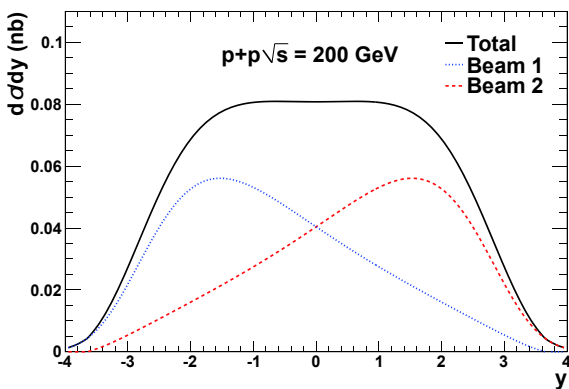


Fig. 3. (color online) The rapidity distribution, $d\sigma/dy$, of J/ψ from photoproduction in NSD p+p collisions at $\sqrt{s} = 200$ GeV. The solid line is the total production, while the dashed/dotted lines represent the individual cross-section contributions from the two beams.

rapidity distribution is determined by the evolution of the photon flux with photon energy ω , and by the elementary γp cross-section at center-of-mass energy $E_{\gamma p}$ at different rapidities.

Figure 4 shows the differential cross-section of J/ψ from hadronic production and photoproduction as a function of rapidity in p+p collisions at $\sqrt{s} = 0.2$ (a), 2.76 (b), 5.02 TeV (c), and 14 TeV (d), respectively. The red and blue dashed lines are predictions from photoproduction with and without interference effect, respectively. The effect of interference will be discussed in detail later. The calculations are performed for NSD collisions, in which violent strong interactions exist that produce J/ψ . The black solid lines with gray bands in the plots represent J/ψ cross-sections from hadronic production. The hadronic contributions are extracted from the parametrizations using the world-wide experimental data, as described in Ref. [40]. The rapidity distributions from photoproduction are different at different collision energies due to the evolution of the two component structures (shown in Fig. 3), and the interference from the two beams. In comparison with the contribution from hadronic interactions, the yield from photoproduction is several orders of magnitude smaller, which makes the detection of J/ψ photoproduction in NSD p+p collisions very difficult.

Could we observe an excess of J/ψ at low p_T in NSD p+p collisions, similar to those in peripheral A+A collisions? Although the total cross-section from photoproduction is very small in comparison to the hadronic contribution, J/ψ from photoproduction are mainly produced at low p_T , which may have certain significance. p_T of J/ψ from photoproduction in p+p collisions depends on p_T of the photon and p_T acquired when the vector meson is created; the latter is dominant. p_T of the photon induced by a proton can be given by the equivalent photon approximation [14]:

$$\frac{d^2 N_\gamma}{d^2 \vec{k}_{\gamma\perp}} = K_0 \frac{F_\gamma^2(\vec{k}_\gamma) \vec{k}_{\gamma\perp}^2}{(\vec{k}_{\gamma\perp}^2 + \omega_\gamma^2/\gamma^2)^2}, \quad (12)$$

where $F_\gamma(\vec{k}_\gamma)$ is the proton form-factor used previously, K_0 is the dimensionless normalization factor, and $\vec{k}_{\gamma\perp}$ is the transverse momentum of the photon. p_T from the vector meson production can be estimated from the world-wide p_T differential cross-section measurements. The measured p_T distributions can be phenomenologically described by:

$$\frac{d\sigma}{dp_T} = N_0 p_T e^{-bp_T}, \quad (13)$$

where N_0 is the normalization factor, b is the slope parameter depending on the γp center-of-mass energy ($E_{\gamma p}$). Figure 5 shows the slope parameter (b) of exclusive J/ψ photoproduction as a function of $E_{\gamma p}$ from the world-

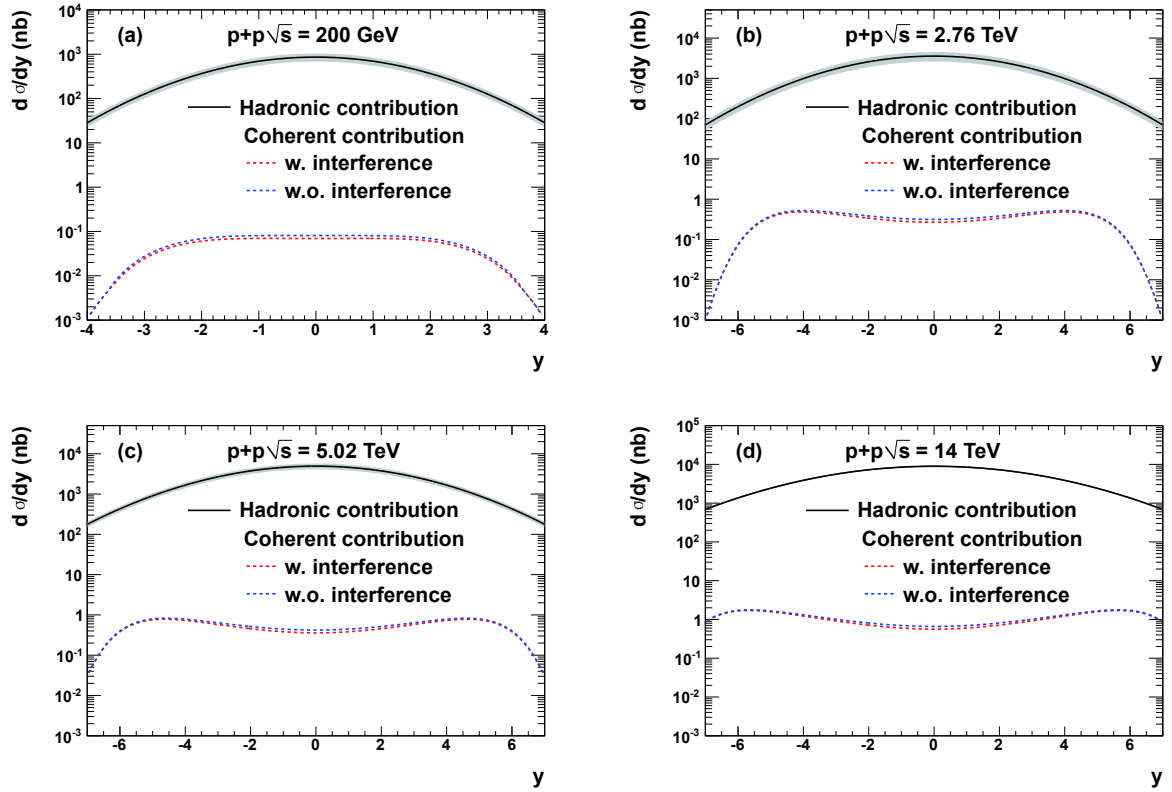


Fig. 4. (color online) The differential cross-section of J/ψ from hadronic production and photoproduction as a function of rapidity in p+p collisions at $\sqrt{s} = 0.2$ (a), 2.76 (b), 5.02 TeV (c), and 14 TeV (d). The red and blue dashed lines are predictions from photoproduction with and without interference effect, respectively. The black solid lines with gray bands represent cross-sections from hadronic production. The hadronic contributions are from parametrizations in Ref. [40].

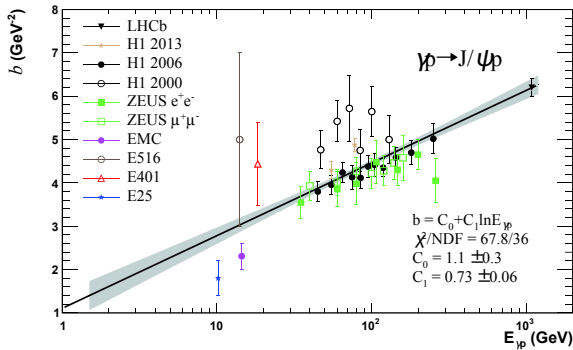


Fig. 5. (color online) The slope parameter (b) of exclusive J/ψ photoproduction as a function of $E_{\gamma p}$ from the worldwide experimental measurements. The black solid line with gray band represents the parametrization discussed in the text.

wide measurements. The references of the data are summarized in Table 1. The black solid line with gray band represents the parametrization discussed below. Within the framework of Regge phenomenology [41], the slope parameter b should increase logarithmically with $E_{\gamma p}$. Therefore, the data are fitted using the following expression:

$$b = C_0 + C_1 \ln E_{\gamma p}, \quad (14)$$

where C_0 and C_1 are free parameters. The corresponding $E_{\gamma p}$ is uniquely determined by the rapidity of J/ψ and the pp collision energy. As shown in the figure, this expression describes the data reasonably well. We assume that the photon p_T and that from the vector meson production are randomly oriented.

For $p_T < \hbar/b$, it is impossible to distinguish which proton emits the photon and which acts as a target. Due to the negative parity of J/ψ , the sign of the two amplitudes are opposite, leading to destructive interference. The interference of vector meson production in UPC has been studied in detail by Klein and Nystrand [42]. We follow the same strategy to calculate the effect of interference:

$$\sigma(p_T, y, b) = A^2(p_T, y, b) + A^2(p_T, -y, b) - 2A(p_T, y, b)A(p_T, -y, b) \times \cos(\vec{p}_T \cdot \vec{b}), \quad (15)$$

where $A(y, p_T, b)$ is the amplitude for J/ψ production at rapidity y with transverse momentum p_T .

Figure 6 shows the differential invariant cross-section of J/ψ from hadronic production and photoproduction as a function of transverse momentum in p+p collisions for mid-rapidity ($|y| < 1$) at $\sqrt{s} = 0.2$ (a), 2.76 (b), 5.02 TeV (c), and 14 TeV (d), respectively. The interference effect has been incorporated in the calculations of

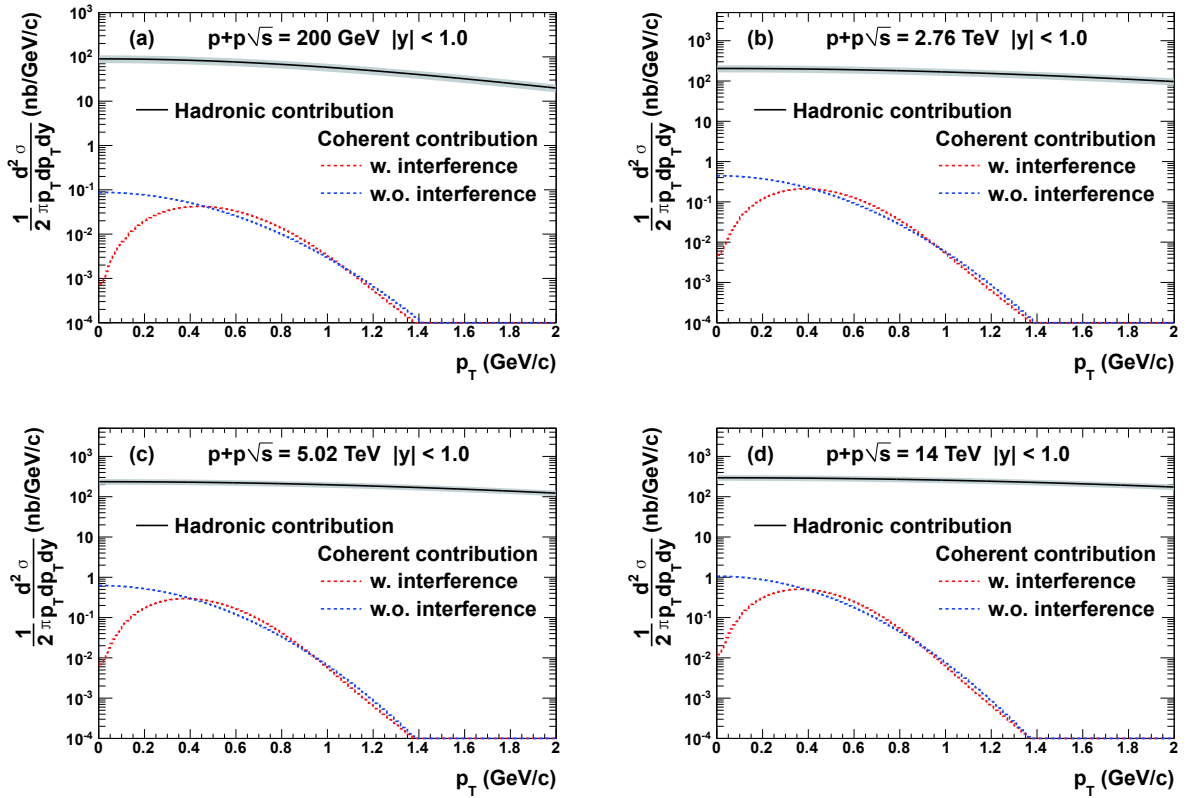


Fig. 6. (color online) The differential invariant cross-section of J/ψ from hadronic production and photoproduction as a function of transverse momentum in p+p collisions for mid-rapidity ($|y| < 1.0$) at $\sqrt{s} = 0.2$ (a), 2.76 (b), 5.02 TeV (c), and 14 TeV (d). The red and blue dashed lines are predictions from photoproduction with and without interference effect, respectively. The black solid lines with gray bands represent cross-sections from hadronic production. The hadronic contributions are from parametrizations in Ref. [40].

photoproduction. The red and blue dashed lines are predictions from photoproduction with and without interference effect, respectively. The black solid lines with gray bands represent cross-sections from hadronic production. The hadronic contributions are extracted from the parametrizations using the world-wide experimental data, as described in Ref. [40]. As depicted in the figure, the photoproduction contribution is several orders of magnitude smaller than from hadronic interactions, which means that the excess from photoproduction at low p_T is not visible in NSD p+p collisions at the RHIC and LHC energies. Why is this the case? The photoproduction of J/ψ is proportional to $Z^2 A^2$, which means that the photoproduction in p+p is $1/Z^2 A^2$ of that in A+A collisions. The form-factor difference between p and A compensates the gap between p+p and A+A up to a certain extent, but it is not enough. For hadronic production, the production in p+p collisions is $1/N_{\text{coll}}$ of that in A+A collisions, where N_{coll} ranges from 1 to 1000 depending on the collision species and centralities. Thus, the contribution from J/ψ photoproduction is negligible in comparison with that from hadronic production. However, this is good news for the current R_{AA} measurements for very low p_T in A+A collisions at RHIC and LHC, since the pp baseline for such a

p_T region comes from extrapolations from the relatively high p_T measurements, which ignore the possible excess originating from photoproduction. The coherent photoproduction contribution could be increased by selecting events with a low charged particle multiplicity [43]. However, there are difficulties in relating the event multiplicity to the impact parameter distribution in p+p collisions, which needs to be further explored in a future work.

4 Conclusion

In summary, we performed a calculation of exclusive J/ψ photoproduction in NSD p+p collisions at the RHIC and LHC energies. The differential rapidity and transverse momentum distributions of J/ψ from photoproduction were presented. In comparison with the J/ψ production from hadronic interactions, the contribution of photoproduction is negligible, which suggests that, in contrast with peripheral A+A collisions, the excess of J/ψ yield from photoproduction is not visible in NSD p+p collisions.

We thank Dr. Spencer Klein and Prof. Pengfei Zhuang for useful discussions.

References

- 1 P. Braun-Munzinger and J. Stachel, *Nature*, **448**: 302 (2007)
- 2 L.-H. Song, L.-W. Yan, and Y. Liu, *Nuclear Science and Techniques*, **29**: 159 (2018)
- 3 X. Luo and N. Xu, *Nuclear Science and Techniques*, **28**: 112 (2017)
- 4 H.-M. Wang et al, *Nuclear Science and Techniques*, **29**: 2911602 (2018)
- 5 T. Matsui and H. Satz, *Physics Letters B*, **178**: 416 (1986)
- 6 C. A. Bertulani, S. R. Klein, and J. Nystrand, *Annual Review of Nuclear and Particle Science*, **55**: 271 (2005)
- 7 V. Rebyakova, M. Strikman, and M. Zhalov, *Physics Letters B*, **710**: 647 (2012)
- 8 K. Eskola, H. Paukkunen, and C. Salgado, *Journal of High Energy Physics*, **2009**: 065 (2009)
- 9 J. Adam et al (ALICE), *Physical Review Letters*, **116**: 222301 (2016)
- 10 W. Zha, *Journal of Physics: Conference Series*, **779**: 012039 (2017)
- 11 M. Klusek-Gawenda and A. Szczurek, *Physical Review C*, **93**: 044912 (2016)
- 12 W. Zha et al, *Physical Review C*, **97**: 044910 (2018)
- 13 W. Shi, W. Zha, and B. Chen, *Physics Letters B*, **777**: 399 (2018)
- 14 F. Krauss, M. Greiner, and G. Soff, *Progress in Particle and Nuclear Physics*, **39**: 503 (1997)
- 15 P. J. Mohr, B. N. Taylor, and D. B. Newell, *Reviews of Modern Physics*, **80**: 633 (2008)
- 16 M. G. Ryskin, *Zeitschrift für Physik C Particles and Fields*, **89**: 57 (1993)
- 17 B. Abelev et al (ALICE), *Physical Review Letters*, **113**: 232504 (2014)
- 18 S. Acharya et al. (ALICE), (2018), arXiv: 1809.03235.
- 19 R. Aaij et al (LHCb), *Journal of Physics G: Nuclear and Particle Physics*, **41**: 055002 (2014)
- 20 R. Aaij et al (LHCb), (2018), arXiv: 1806.04079
- 21 C. Alexa et al (H1), *The European Physical Journal C*, **73**: 2466 (2013)
- 22 A. Aktas et al (H1), *The European Physical Journal C*, **46**: 585 (2006)
- 23 C. Adloff et al (H1), *Physics Letters B*, **483**: 23 (2000)
- 24 S. Chekanov et al (ZEUS), *The European Physical Journal C*, **24**: 345 (2000)
- 25 J. Aubert et al, *Physics Letters B*, **89**: 267 (1980)
- 26 A. R. Clark et al, *Physical Review Letters*, **45**: 682 (1980)
- 27 A. R. Clark et al, *Physical Review Letters*, **43**: 187 (1979)
- 28 B. H. Denby et al, *Physical Review Letters*, **52**: 795 (1984)
- 29 M. Binkley et al, *Physical Review Letters*, **48**: 73 (1982)
- 30 B. Knapp et al, *Physical Review Letters*, **34**: 1040 (1975)
- 31 S. D. Holmes, W. Lee, and J. E. Wiss, *Annual Review of Nuclear and Particle Science*, **35**: 120185 (1985)
- 32 T. Nash et al, *Physical Review Letters*, **36**: 1233 (1976)
- 33 U. Camerini et al, *Physical Review Letters*, **35**: 483 (1975)
- 34 B. Gittelman et al, *Physical Review Letters*, **35**: 1616 (1975)
- 35 M. Tanabashi et al (Particle Data Group), *Physical Review D*, **98**: 030001 (2018)
- 36 V. Guzey, E. Kryshen, M. Strikman et al, *Physics Letters B*, **726**: 290 (2013)
- 37 W. Zha et al, (2018), arXiv: 1810.02064
- 38 S. R. Klein and J. Nystrand, *Physical Review C*, **60**: 014903 (1999)
- 39 B. Abelev et al (ALICE), *The European Physical Journal C*, **73**: 2456 (2013)
- 40 W. Zha et al (ALICE), *The European Physical Journal C*, **93**: 024919 (2016)
- 41 P. D. B. Collins, *An Introduction to Regge Theory and High-Energy Physics*, Cambridge Monographs on Mathematical Physics (Cambridge Univ. Press, Cambridge, UK, 2009)
- 42 S. R. Klein and J. Nystrand, *Physical Review Letters*, **84**: 2330 (2000)
- 43 B. Abelev et al (ALICE), *Physics Letters*, **712**: 165 (2012)